



ELSEVIER

Contents lists available at ScienceDirect

Ultrasonics - Sonochemistry

journal homepage: www.elsevier.com/locate/ultson

Sonochemical coating of Prussian Blue for the production of smart bacterial-sensing hospital textiles

Amparo Ferrer-Vilanova^{a,*}, Yasmine Alonso^b, Jiri Dietvorst^a, Marta Pérez-Montero^c, Rosalía Rodríguez-Rodríguez^c, Kristina Ivanova^d, Tzanko Tzanov^d, Núria Vigués^e, Jordi Mas^e, Gonzalo Guirado^b, Xavier Muñoz-Berbel^a

^a Instituto de Microelectrónica de Barcelona (IMB-CNM, CSIC), Carrer dels Til·lers s/n, Campus Universitat Autònoma de Barcelona, 08193, Cerdanyola del Vallès, Barcelona, Spain

^b Departament de Química, Universitat Autònoma de Barcelona, 08193, Cerdanyola del Vallès, Barcelona, Spain

^c Basic Sciences Department, Faculty of Medicine and Health Sciences, Universitat Internacional de Catalunya, 08195, Sant Cugat del Vallès, Barcelona, Spain

^d Universitat Politècnica de Catalunya, Edifici Gaia, Pg. Ernest Lluch/Rambla Sant Nebridi s/n. 08222, Terrassa, Barcelona, Spain

^e Departament de Genètica i Microbiologia, Universitat Autònoma de Barcelona, 08193, Cerdanyola del Vallès, Barcelona, Spain

ARTICLE INFO

Keywords:

Sonochemical coating
Smart textiles
Bacterial detection
Prussian Blue
Metabolic indicators
Hospital acquired infections

ABSTRACT

In healthcare facilities, environmental microbes are responsible for numerous infections leading to patient's health complications and even death. The detection of the pathogens present on contaminated surfaces is crucial, although not always possible with current microbial detection technologies requiring sample collection and transfer to the laboratory. Based on a simple sonochemical coating process, smart hospital fabrics with the capacity to detect live bacteria by a simple change of colour are presented here. Prussian Blue nanoparticles (PB-NPs) are sonochemically coated on polyester-cotton textiles in a single-step requiring 15 min. The presence of PB-NPs confers the textile with an intensive blue colour and with bacterial-sensing capacity. Live bacteria in the textile metabolize PB-NPs and reduce them to colourless Prussian White (PW), enabling in situ detection of bacterial presence in less than 6 h with the bare eye (complete colour change requires 40 h). The smart textile is sensitive to both Gram-positive and Gram-negative bacteria, responsible for most nosocomial infections. The redox reaction is completely reversible and the textile recovers its initial blue colour by re-oxidation with environmental oxygen, enabling its re-use. Due to its simplicity and versatility, the current technology can be employed in different types of materials for control and prevention of microbial infections in hospitals, industries, schools and at home.

1. Introduction

“Nosocomial” or “hospital-acquired infections” (HAI) are infections that the patient acquires in the hospital or healthcare facility from microbes present in the environment. The main means of transmission include the direct physical contact of the patient with a contaminated surface or element, either the skin (of the healthcare personnel or the own patient), aerosols, shared instruments, furniture or hospital fabrics. Recently, pathogenic bacteria have been identified in hospital textiles [1,2], but, in practice, there is no way of knowing if a textile in use is contaminated or not. Therefore, to minimize the impact of nosocomial infections in hospitalized patients it is crucial to detect the presence of

microbes on contaminated surfaces in situ and within a reasonable period of time.

Microbial detection is currently possible in the laboratory with a number of dedicated techniques and instruments, the most common being cell culture imaging [3,4], or sequencing [5,6], polymerase chain reaction (PCR) [7] and enzyme-linked immunosorbent assay (ELISA) [8]. With these techniques, samples are collected, transported to the laboratory and analysed using tedious and long protocols, impossible to be implemented as a routing warning system. As a step forwards, a number of biosensors have been developed based on the previous systems where bacteria are identified through selective DNA strains (DNA-sensors) [9] or antigens/antibodies (immune-sensors) [10]. Portable

* Corresponding author.

E-mail addresses: amparo.ferrer@imb-cnm.csic.es (A. Ferrer-Vilanova), yasminee95@gmail.com (Y. Alonso), jiri.dietvorst@imb-cnm.csic.es (J. Dietvorst), mperez@uic.es (M. Pérez-Montero), rrodriguez@uic.es (R. Rodríguez-Rodríguez), kristina.ivanova@upc.edu (K. Ivanova), tzanko.tzanov@upc.edu (T. Tzanov), nuria.vigues@uab.cat (N. Vigués), jordi.mas@uab.cat (J. Mas), gonzalo.guirado@uab.cat (G. Guirado), xavier.munoz@imb-cnm.csic.es (X. Muñoz-Berbel).

<https://doi.org/10.1016/j.ultsonch.2020.105317>

Received 8 April 2020; Received in revised form 2 July 2020; Accepted 23 August 2020

Available online 27 August 2020

1350-4177/ © 2020 Elsevier B.V. All rights reserved.

systems have been developed based on the latter [11,12], although they still requiring sample collection and sometimes concentration/amplification before analysis. Hence, these technologies are still difficult to implement in situ. This is partially tackled by the use of metabolic indicators. Metabolic indicators are molecules that change their properties when metabolized by microorganisms. The sensing strategy varies depending on the indicator but they are mostly based on changes of pH (bacterial metabolism reduces pH) [13] or conductivity (bacterial metabolism tends to increase medium conductivity) [14], ATP production [15] or reduction of redox molecules by proteins and/or mediators from the metabolic electron transport chain [16,17]. Although in most cases they are used as laboratory reagents, many kits containing these compounds for in situ identification of contaminated surfaces have been developed [18]. The solution with the indicator is sprayed on the potentially contaminated surface and an optical change is produced, which can be associated to the presence of living bacteria. This optical change is normally a colour appearance/disappearance (for pH, conductivity or redox state) or fluorescence production (in the case of ATP). Contaminated surfaces are thus identified using a simple and fast protocol, with the main limitation of requiring dedicated personnel and equipment to analyse the huge number of potentially risky surfaces and elements present in a hospital.

In the current work, an equipment-free alternative for in situ determination of bacterial contamination is presented based on the incorporation of the sensing metabolic indicators in the surface of interest, in this case hospital fabrics, through a single-step sonochemical coating process. Sonochemical coating of hospital textiles has been widely explored by some groups in the recent years. Gedanken's and Tzanov's groups have successfully implemented metal nanoparticles (NPs), metal oxide-NPs and/or enzymes on textiles for the production of antibacterial hospital fabrics [19–22]. Also metal-oxides and dyes could be co-deposited in a single sonochemical coating process [23]. In the present study, sonochemical coating is employed to incorporate iron-based complexes in the textile for the production of smart bacterial-sensing hospital fabrics. Ferric hexacyanoferrate NPs, also known as Prussian Blue (PB), has been selected since, apart from being a well-known textile dye [24], it presented ideal properties, such as: (i) a sufficiently high redox potential, able to react with proteins and mediators from the bacterial electron transport chain [25]; (ii) high extinction molar coefficients and an evident colour change after reduction, even visible to the naked eye [26,27]; (iii) biocompatibility [28–30]; and (iv) existing preliminary results supporting its use as metabolic indicator by bacterial reduction [31]. The possibility of using the metabolic conversion from PB to its reduced form, Prussian White (PW) as early warning system for contaminated surface identification is evaluated in this paper. The sonochemical implementation of PB-NPs is studied and optimized to obtain sensitive smart bacterial-sensing fabrics with a homogeneous colour distribution and through a simple protocol. The sensing capacity of the final smart fabric is tested using *Escherichia coli* (*E. coli*) and *Staphylococcus aureus* (*S. aureus*) samples, used as model for Gram-negative and Gram-positive bacteria, respectively.

2. Materials and methods

2.1. Reagents

Potassium ferricyanide ($K_3[Fe(CN)_6]$), iron(II) chloride ($FeCl_2$), hydrogen chloride (HCl 37%), 2-(N-morpholino)ethane-sulfonic acid hydrate (MES hydrate), 2-hydroxyethyl cellulose with an average molecular mass of 380 kDa and Dulbecco's Modified Eagle's Medium (DMEM, supplemented with 10% fetal bovine serum, 1% penicillin/streptomycin solution) were purchased from Sigma-Aldrich (Spain). Iron (III) chloride anhydrous ($FeCl_3$) was obtained from Fischer Scientific. Glucose, sodium borohydride ($NaBH_4$), potassium phosphate dibasic trihydrate ($K_2HPO_4 \cdot 3H_2O$) and potassium dihydrogen

phosphate (KH_2PO_4) were from Panreac (Spain). Potassium chloride (KCl) and oxalic acid were purchased from Probus. All chemicals were used as received. Aqueous solutions were prepared using de-ionized water.

2.2. Synthesis of PB-NPs

Depending on the counter-ion used for charge compensation, two forms of PB can be synthesized: the "soluble" PB (PB_{sol}), which incorporates potassium as counter-ion, and the "insoluble" PB (PB_{ins}) containing iron ions as counter ions. Both PB forms present important structural and functional differences, e.g. in the deposition kinetics. That is, while PB_{sol} -NPs present slow deposition kinetics by the small size of the particles, PB_{ins} -NPs, containing aggregations of NPs, precipitate quickly [28,32,33].

PB-NPs were synthesized by a chemical reaction of ferric and hexacyanoferrate ions in aqueous solution (i.e. water) until a dark blue colloid is formed [33,34]. For PB_{sol} synthesis, equimolar solutions (30 mM) of $FeCl_2$ and $K_3[Fe(CN)_6]$ were used. Concretely, 25 mL of the ferricyanide solution were added dropwise to 25 mL of iron dichloride resulting in a dark blue solution corresponding to PB_{sol} . On the other hand, PB_{ins} was synthesized by mixing 50 mL of 15 mM $K_3[Fe(CN)_6]$ with an excess of $FeCl_2$ (30 mL of a 0.1 M solution). In this case, however, it was the iron dichloride solution which was added dropwise to the ferricyanide producing the formation of the dark blue precipitate corresponding to the PB_{ins} formation. The precipitate was left to deposit and cleaned twice with distilled water. As previously demonstrated, light can affect PB-NPs stability [35], hence synthesized nanoparticles were stored protected from light until used.

2.3. Sonochemical coating of polyester-cotton textiles with PB-NPs

Polyester-cotton fabrics (KLOPMAN, Italy) from industrial production of hospital pyjamas were used as model hospital textiles. The sonochemical coating process was performed employing an ultrasonic transducer (Ti-horn, 20 kHz, 750 W, Sonics and Materials CV334, USA), as illustrated in Fig. 1a. The power (21.5 W) and intensity (0.43 W/cm³) were determined calorimetrically by measuring the temperature increase in the ultrasonic vessel as detailed in [36]. Polyester-cotton fragments (3 × 3 cm; approx. 0.18 g) were immersed in the ultrasonic pot already containing 50 mL of the PB-NPs aqueous suspension. In the optimization of the sonochemical coating process, PB at concentrations from 0.03 to 0.3 mM and sonication times of 5, 15 and 30 min were evaluated at a temperature of 20 °C and the amplitude was kept at 35%. This amplitude was high enough to provide textiles with a homogeneous distribution of NPs, resulting in colour homogeneity, but without compromising the integrity of the textile. Higher amplitudes were observed to produce textile damage.

2.4. Spectroelectrochemical analysis of the smart textiles

The electrochromic behaviour of PB-NPs was studied after their deposition on polyester-cotton fabrics. Spectroelectrochemical analysis was performed using a sandwich configuration spectroelectrochemical cell. Platinum electrodes were located in front of the PB-coated textiles, with a solid hydrogel electrolyte layer in between, which allowed the study of solid materials without the need of solvents. In this case, 2-hydroxyethyl cellulose was used as solid electrolyte. Cellulose-based electrolytes were prepared by dissolving 2-hydroxyethyl cellulose (380 kDa) in 1 M KCl to a final concentration of 6.5% (w/v). Reagents were mixed under magnetic stirring, increasing the temperature until boiling. The solution was then left to dry at room temperature. Electrochemical measurements were performed with a potentiostat PAR biologic, SA, VSP100 (BAS Inc. Tokyo) controlled by the EC-Lab V9.51 software (BAS Inc., Tokyo). Simultaneous optical records were acquired with a Hamamatsu L10290 spectrophotometer (Hamamatsu, Japan)

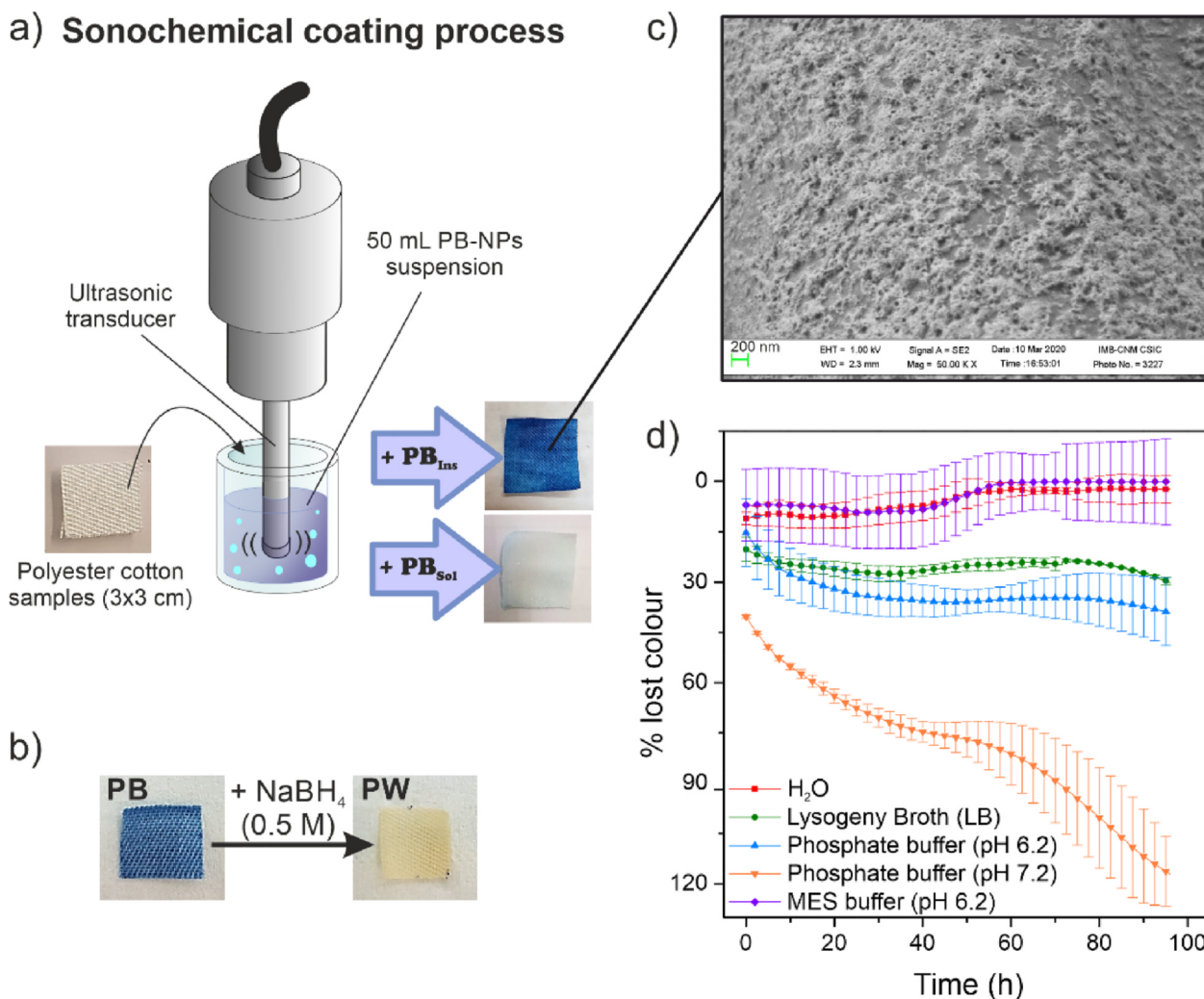


Fig. 1. Sonochemical coating process and characterization of PB-modified textiles. (a) Scheme of the sonochemical coating process and resulting textiles obtained after incorporation of PB_{sol} or PB_{ins}. (b) SEM image of the samples modified with PB_{ins} 0.08 mM. (c) PB-modified textile reduced to PW after addition of NaBH₄ 0.5 M as reducing agent. (d) Colour stability of polyester-cotton textiles modified with PB_{ins} 0.08 mM after 96 h submerged in (i) water, (ii) LB, 0.1 M phosphate buffered saline (PBS) at (iii) pH 6.2 and (iv) pH 7.2, and (v) 0.1 M MES buffer (pH 6.2), all supplemented with 0.1% glucose. Lost colour was expressed as percentage versus unmodified textiles colour ($n = 3$).

controlled by the Bio-Kine 32 V4.46 software (BAS Inc. Tokyo).

2.5. SEM measurements

The surface topology of the PB-modified textiles was studied by scanning electron microscopy (SEM) using an AURIGA® series en04 SEM (CarlZeiss).

2.6. Bacterial cultures preparation

Escherichia coli (ATCC 25922) (*E. coli*) and *Staphylococcus aureus* (ATCC 29213) (*S. aureus*) were used as model Gram-negative and Gram-positive bacteria, respectively. Both bacteria were incubated aerobically in a Luria-Bertani (LB) broth overnight (18 h) at 37 °C with shaking. After centrifugation (Eppendorf centrifuge AG R134A) at 2700xg for 10 min, the pellet was collected and re-suspended in 0.1 M MES (pH 6.2) adjusting bacterial concentration through optical density measurements in a spectrophotometer (Smartspec™ Plus spectrophotometer, Bio-rad, California, US). An optical density of 0.1 A.U. was considered equivalent to 10⁸ colony forming units per mL (CFU mL⁻¹). Suitable aliquots were cultured in agar plates and counted after incubation for adjustment of bacterial concentration.

2.7. Evaluation of bacterial-sensing activity of smart textiles incorporating PB-NPs

To study the bacterial-sensing capacity of the PB-modified textiles, polyester-cotton fabrics (1 × 1 cm, approx. 0.02 g) modified with 0.08 mM PB_{ins} were incubated in bacterial suspensions (from 10⁵ to 10⁹ CFU mL⁻¹) in (i) water, (ii) LB, 0.1 M phosphate buffered saline (PBS) at (iii) pH 6.2 and (iv) pH 7.2, and (v) 0.1 M MES buffer (pH 6.2), all of them supplemented with 0.1% glucose. Samples were always analysed during the first 15 days of preparation to ensure repeatability of the results. Colour changes were monitored in real time with a digital microscope camera DigiMicro 2.0 Scale for five days. Selected images were analysed using the freeware *ImageJ*. The three RGB channels were separated choosing the red one for quantification since it was the most sensitive. The percentage of colour lost was calculated by comparing it with the initial colour of the unmodified polyester-cotton textile.

2.8. Cytotoxicity evaluation

PB cytotoxicity was determined in the human fibroblast cell line MRC-5 (ATCC Line Bank, Virginia, USA) by using the colorimetric MTT (3-(4,5-dimethylthiazol-2-yl)-2,5-diphenyltetrazolium bromide) assay.

a) Spectroelectrochemical set-up

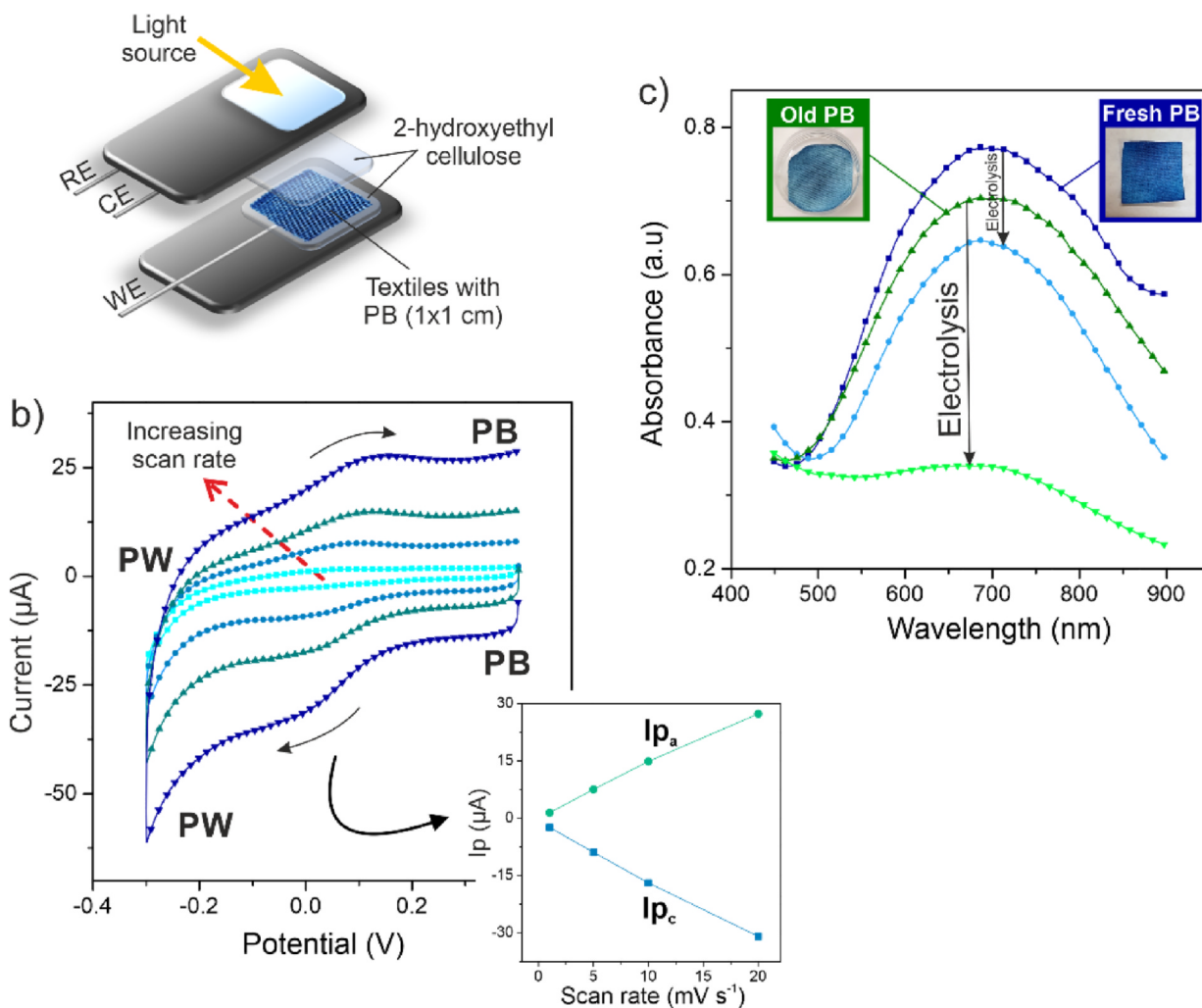


Fig. 2. Spectroelectrochemical measurements on the modified textiles. (a) Set-up scheme used for the spectroelectrochemical measurements on the textiles. (b) CVs of PB-modified textiles developed between 0.4 and -0.3 V at different scan rates (1, 5, 10 and 20 mV s^{-1}) and representation of current peak values obtained vs scan rate. (c) Comparative spectra obtained from textiles coated with PB_{Ins} freshly prepared and PB_{Ins} prepared 4 days before the coating process and corresponding spectra after apply -0.5 V during 15 min to each one of them.

The protocol was based on a previous publication [37]. Briefly, MRC-5 cells were cultured in complete Dulbecco's Modified Eagle's Medium (DMEM, supplemented with 10% foetal bovine serum, 1% penicillin/streptomycin solution). When confluent, cells were exposed to different concentrations of PB_{Sol} and PB_{Ins} . After 24 h of incubation, wells were washed with PBS, and the MTT solution (5 mg mL^{-1}) was added and incubated for 1 h (37°C , 5% CO_2). After washing with PBS, the purple formazan generated by MTT metabolism of viable cells was solubilized with DMSO. The optical density of each well was determined at 570 nm in a spectrophotometer reader (BioTek® Synergy HT, Vermont, USA). Cell viability was expressed as percentage in relation to non-treated cells.

3. Results and discussion

3.1. Sonochemical coating and characterization of the smart textiles

PB was selected as bacterial-sensing probe in the development of the smart textiles, based on previously reported results demonstrating its potential as metabolic bacterial indicator [31]. In the sonochemical coating of PB-NPs, high-intensity ultrasound is applied to the NPs

suspension. High-intensity ultrasound is a simple, fast, efficient and environmentally friendly approach for surface functionalization. Under ultrasound high-speed microjets are generated upon the implosive collapse of bubbles formed in the liquid, the so-called cavitation phenomenon. These microjets project the NPs found in the vicinity of the collapsing bubbles towards the textiles forming stable and homogeneous coatings [22,36,38,39].

In this work, polyester-cotton samples ($3 \times 3 \text{ cm}$) were immersed in aqueous suspensions of PB-NPs and sonochemically coated varying the sonication time (from 5 to 30 min), PB type (PB_{Sol} or PB_{Ins}) and concentration (from 0.03 to 30 mM) (Fig. S1). From the two forms of PB, only PB_{Ins} was stably incorporated in the textile, while PB_{Sol} was almost completely removed after a soft cleaning process by rinsing with buffer (Fig. 1a). Also, the ageing of the PB_{Ins} suspension influenced the sonochemical coating. Freshly prepared samples presented more homogeneity and colour intensity than their 4-days old counterparts (Fig. S2). Homogeneous and highly-coloured samples were obtained after coating with freshly-prepared PB suspensions containing 0.08 mM PB for at least 15 min of sonication. No relevant changes were observed when longer sonication times were applied. SEM image of this sample revealed homogeneously distributed, although sometimes aggregated,

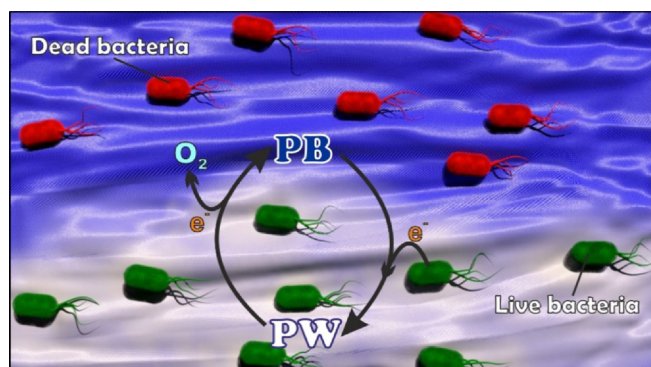


Fig. 3. Scheme of the smart textile behaviour when in contact with live and dead bacteria. Living bacteria are represented in green colour and the dead one in red. (For interpretation of the references to colour in this figure legend, the reader is referred to the web version of this article.)

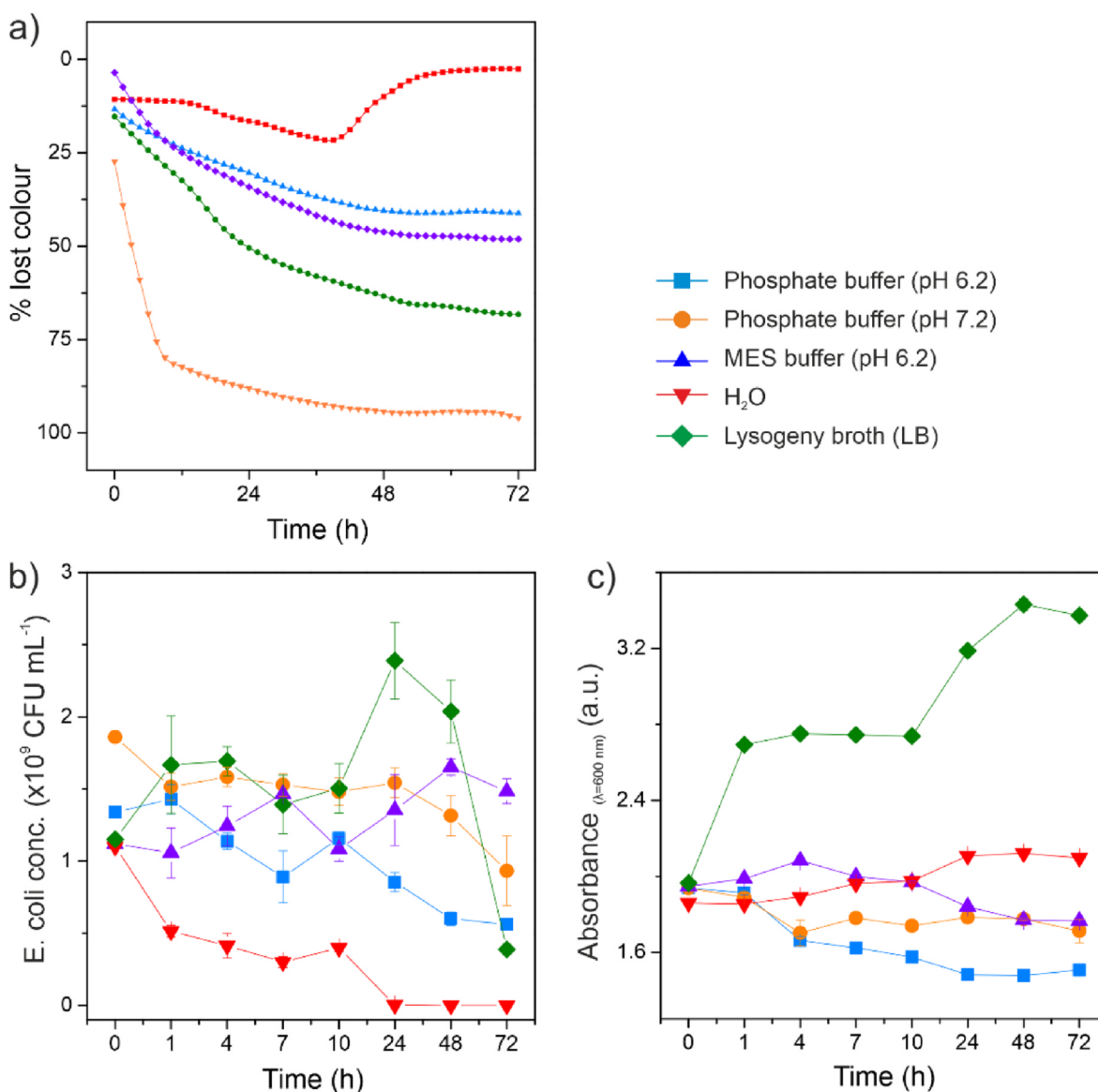


Fig. 4. Relation between bacterial-sensing capacity of the textiles and bacterial proliferation. Different parameters obtained after PB-NPs modified textiles were incubated with *E. coli* for 72 h, such as (a) textile loss of colour percentage; (b) *E. coli* concentration by cell counting and (c) absorbance values at 600 nm throughout the experiment. *E. coli* concentrations above 10^9 CFU mL⁻¹ in 900 μL were incubated in different media (H₂O, LB, 0.1 M PBS (at pH 6.2 and 7.2) and 0.1 M MES (pH 6.2)) and 0.1% of glucose was used (n = 3). A common legend for all the graphs is on top.

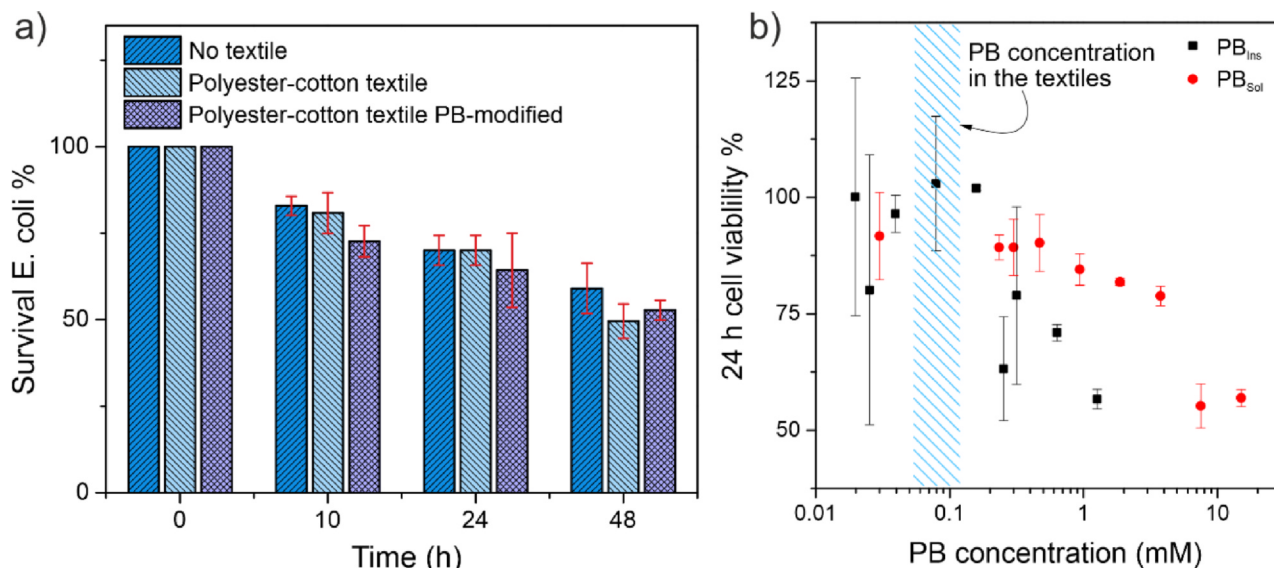


Fig. 5. Antibacterial activity of PB-modified textiles and cytotoxicity. (a) Survival percentage of *E. coli* measured at different incubation times for polyester-cotton textiles with and without PB in MES 0.1 M medium at pH 6.2 and with 0.1% of glucose. As control, an inoculated solution in the same medium without textile sample was used ($n = 3$). (b) MTT cytotoxicity assay for PB_{sol} (red circles) and PB_{ins} (black squares) solutions at different concentrations. Concentrations are represented in a logarithmic scale and the one used in the textiles (0.08 mM PB) is highlighted in the graph with blue cross lines. Cell viability was determined after 24 h of incubation with both solutions ($n = 3$) and viability was expressed as percentage versus non-treated control samples. (For interpretation of the references to colour in this figure legend, the reader is referred to the web version of this article.)

from the pH, the medium composition also had a role in the stability of PB-NPs. Coated samples were more stable in MES than in PBS, even when both buffers had the same pH (pH 6.2). The reason for that may be in the monovalent ions content, e.g. sodium and potassium, which is much higher in PBS than in MES. The presence of such ions, which may substitute iron as counterions in the PB structure, might reduce the stability of NPs incorporated in the textile. In fact, overnight incubation of the textiles with KCl, LiCl or $NaNO_3$ led to the dissociation of the PB and colour disappearance (Fig. S3). LB medium, slightly acidic and with monovalent ions in its composition, maintained around 70% of the initial colour similarly to PBS at pH 6.2. On the other hand, distilled water, acidic on its own but without important concentration of monovalent counter ions, presented low colour losses comparable to MES. Therefore, both ionic composition and pH influenced the stability of PB-NPs incorporated in the textile, but pH-mediated PB decomposition presented faster dissolution kinetics.

The reversibility of PB-NPs incorporated in the textile was studied spectroelectrochemically to evaluate structural/compositional changes along reduction/oxidation cycles. A sandwich configuration with a solid electrolyte, i.e. 2-hydroxyethyl cellulose was used to study the activity of the smart textiles without solvents (Fig. 2a). CVs (between 0.4 to -0.3 V) at different scan rates (1, 5, 10 and 20 $mV s^{-1}$) clearly reported two peaks, corresponding to the reduction from PB to PW (at 0 V) and the subsequent re-oxidation of PW to PB at 0.13 V (Fig. 2b). Peak intensities increased directly with the scan rate and the relationship between intensity of the anodic and cathodic peaks was approximately 1, which corresponded to the behaviour of a thin film system [43]. These samples were also very stable to electrolysis. After applying -0.5 V potential for 15 min, the sample only lost 20% of the initial colour. Much more significant colour loss was observed in the case of samples prepared with old PB suspension, which lost more than 90% of colour due to their low stability (Fig. 2c). It confirmed that freshly prepared PB-NPs in textiles were stable and reversible in solid state when monovalent cations were not present in the medium.

3.2. Bacterial-sensing activity of smart textiles

As an already demonstrated metabolic bacterial indicator [31], PB

in the textile should confer it with bacterial-sensing activity through the mechanism illustrated in Fig. 3. Once the sonochemical coating of PB-NPs provides the fabrics with an intense blue colour, the attachment of live bacteria would change the smart fabric colour by the metabolic reduction of PB to PW by proteins (e.g. cytochrome) and mediators (e.g. ubiquinone) from the bacterial electron transport chain [44]. Since the reaction is metabolic, dead bacteria would not be able to produce this change. If live bacteria died, for example by an antibacterial treatment, the atmospheric oxygen would re-oxidize PW to PB [45], and the smart textile would recover its initial blue colour.

Bacterial-sensing capacity of PB-coated textiles was evaluated spectroscopically (as % colour change) in distilled H_2O , LB, PBS (at pH 6.2 and 7.2) and MES buffer (pH 6.2) containing between 10^8 and 10^9 $CFU mL^{-1}$ *E. coli* (Fig. 4a). Since bacterial proliferation depends on the medium composition, the evolution of this parameter over time was determined in each medium through plating (Fig. 4b) and optical density measurements at 600 nm (Fig. 4c).

All modified textiles presented important colour changes over time, stronger than those observed in the stability studies. Three different behaviours were observed depending on the media. First, in LB, bacteria almost doubled the initial concentration in the sample during the experiment, enabling a fast metabolic reduction of PB resulting in a 60% colour loss after 72 h, the largest reported. Second, in buffer, either PBS or MES, bacterial concentration slightly decreased over time, which resulted in weaker colour changes of 40–45%. The higher colour change observed in the PBS sample at pH 7.2 was again attributed to the pH-mediated decomposition of PB. In fact, when set at the same pH, PBS and MES presented very similar colour change kinetics, as well as analogous bacterial concentrations and bacterial proliferation rates. Finally, textiles incubated in distilled water presented an initial colour loss of 30%, followed by a fast colour recovery by oxygen re-oxidation when the bacteria died (which was confirmed by cell counting). Regarding the latter, smart textile reported the presence/absence of living bacteria on real time thanks to its reversibility.

To confirm that PB-NPs detected bacterial activity without affecting microbial structure and/or function, the antibacterial activity of the smart textiles was evaluated. Antibacterial activity was determined by incubation of the samples in *E. coli* suspensions in MES (pH 6.2)

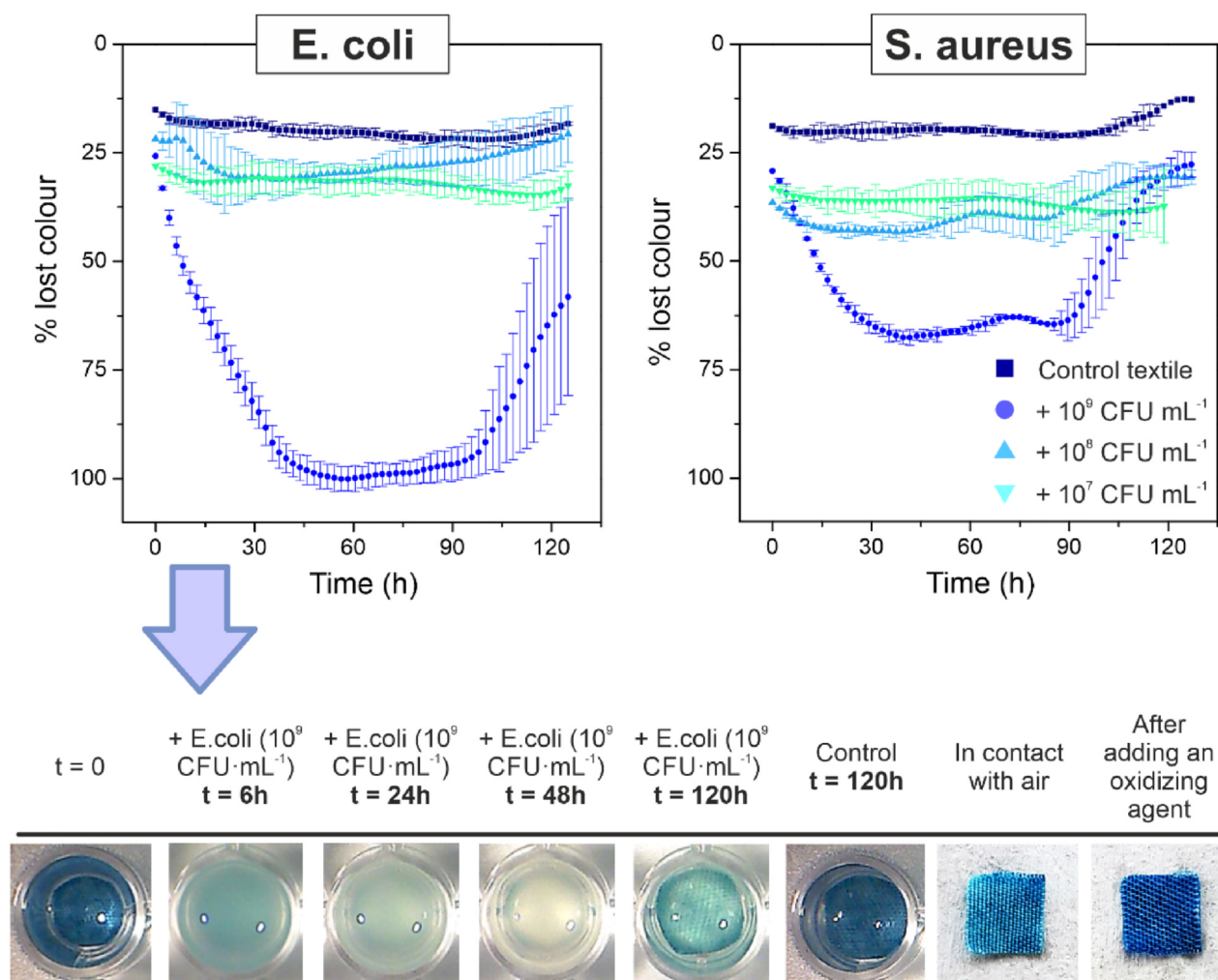


Fig. 6. Bacterial-sensing activity of PB-modified textiles. Quantification of PB-modified textiles colour loss after incubation with *E. coli* and *S. aureus* in MES medium (pH 6.2) and 0.1% of glucose. Bacteria concentrations are shown in a common legend. As control, PB-modified textiles were submerged in MES solution, without bacteria. Colour loss was expressed as percentage versus unmodified-textiles colour ($n = 3$). In the schematic table, representative images from the textiles can be seen at different times of the experiment with *E. coli* inoculation, when they were in contact with air and after adding an oxidizing agent.

supplemented with 0.1% glucose. Modified textiles, non-modified textiles (without PB-NPs) and control samples (bacterial suspension without textile) were studied. The number of viable bacteria was represented as a survival percentage from the initial concentration (Fig. 5a). No significant differences were observed between control, non-modified and modified textiles, confirming the low or null antibacterial activity of the PB-NPs in the textile.

On the other hand, because of the direct physical contact with skin, cytotoxicity assays of PB-NPs were performed to evaluate its potential risk for human health. Fig. 5b shows that both soluble and insoluble PB-NPs were cytotoxic when in high concentrations, with a decrease of the cell viability near to 50%. However, the concentration implemented in the textiles was not cytotoxic and should not represent a risk.

Finally, the capacity to detect different bacterial types was evaluated by comparing the response of the smart textile to the Gram-negative *E. coli* with the Gram-positive *S. aureus* bacteria. Experiments were performed in MES (pH 6.2) with 0.1% of glucose at bacterial concentrations of 10^7 , 10^8 or 10^9 CFU mL⁻¹. Results are summarized in Fig. 6. In both cases, no detectable changes were observed in the control sample (without bacteria) or after 5 days of incubation in bacterial suspension with a concentration below 10^7 CFU mL⁻¹. Textiles incubated with 10^8 CFU mL⁻¹ presented a small colour change that was quickly reversed until it recovered the initial colour. More pronounced and sustained changes were observed after incubation with 10^9 CFU

mL⁻¹, which was even detectable with the bare eye after 6 h of incubation. The complete colour loss required 48 h. In the case of *S. aureus*, the peptidoglycan layer typical in Gram-positive bacteria slows down the extracellular electron transfer to the PB-NPs [46], showing slower kinetics. After 90 h, when most of bacteria in the sample were already dead as result of nutrients depletion, the textiles started to recover their initial blue colour through oxygen re-oxidation. The complete colour recovery required a reaction with an oxidizing agent, i.e. hydrogen peroxide, as shown in the images, confirming the stability of PB-NPs in the textiles.

4. Conclusions

To prevent HAI contamination, a smart hospital fabric able to detect the presence of living bacteria by changing its own colour is developed here based on the incorporation of sensing NPs by sonochemical coating. PB-NPs are chosen as the most suitable metabolic indicator for being able to identify living bacteria by producing an intense and reversible colour change when it is reduced by bacterial metabolism to PW. From the two forms of PB, only freshly-prepared PB_{Ins}-NPs can be sonochemically incorporated in textile with sufficient concentration and homogeneity. Optimal conditions require sonication of 0.08 mM PB-NPs for 15 min in a single-step ultrasonic process. PB-NPs in the textile are not antibacterial or cytotoxic, and maintain the

bacterial-sensing capacity reported in solution both for Gram-positive and Gram-negative bacteria. In the latter case, a detectable colour change is observed after 5–6 h of incubation in high bacterial concentrations (10^9 CFU mL⁻¹), with a total colour change after 40 h. The textile recovers the colour when bacteria die by re-oxidation mediated by environmental oxygen. Thus, these smart textiles allow the detection of live bacteria in situ, which are even detectable by the naked eye. Future efforts are focused on the improvement of the response time and the sensitivity of the technology, either by chemical modification of the probe or by integration of transduction mechanisms. Also, the implementation of the current sonochemical coating protocol in real production lines is now being explored. We envision the current strategy of potential interest in the control of infections in hospitals, industries, schools or at home.

CRedit authorship contribution statement

Amparo Ferrer-Vilanova: Conceptualization, Formal analysis, Investigation, Visualization, Writing - original draft. **Yasmine Alonso:** Validation, Investigation. **Jiri Dietvorst:** Investigation, Writing - review & editing. **Marta Pérez-Montero:** Investigation, Resources. **Rosalía Rodríguez-Rodríguez:** Investigation, Resources, Writing - review & editing. **Kristina Ivanova:** Validation, Investigation, Resources, Writing - review & editing. **Tzanko Tzanov:** Conceptualization, Validation, Project administration. **Núria Vigués:** Investigation, Resources. **Jordi Mas:** Validation, Resources. **Gonzalo Guirado:** Conceptualization, Methodology, Writing - review & editing. **Xavier Muñoz-Berbel:** Conceptualization, Methodology, Writing - original draft, Writing - review & editing, Supervision, Funding acquisition.

Declaration of Competing Interest

The authors declare that they have no known competing financial interests or personal relationships that could have appeared to influence the work reported in this paper.

Acknowledgements

This work was supported the European Commission through the project PROTECT (H2020-NMBP-PILOT-720851). The authors thank the Ministerio de Ciencia e Innovación of Spain for financial support through the projects CTQ 2015-65439-R and PID2019-106171RB-I00.

Appendix A. Supplementary data

Supplementary data to this article can be found online at <https://doi.org/10.1016/j.ultsonch.2020.105317>.

References

- [1] L. Sehulster, R.Y.W. Chinn, Guidelines for environmental infection control in health-care facilities, *Morb. Mortal. Wkly. Rep.* 52 (RR10) (2003) 1–42.
- [2] S. Fijan, S.Š. Turk, Hospital textiles, are they a possible vehicle for healthcare-associated infections? *Int. J. Environ. Res. Public Health* 9 (9) (2012) 3330–3343, <https://doi.org/10.3390/ijerph9093330>.
- [3] T. Zimmermann, J. Rietdorf, R. Pepperkok, Spectral imaging and its applications in live cell microscopy, *FEBS Lett.* 546 (1) (2003) 87–92, [https://doi.org/10.1016/S0014-5793\(03\)00521-0](https://doi.org/10.1016/S0014-5793(03)00521-0).
- [4] M. Arora, Cell culture media: a review, *Mater. Methods* 3 (2013) 1–29, <https://doi.org/10.13070/mm.en.3.175>.
- [5] B.S. Yadav, V. Ronda, D.P. Vashista, B. Sharma, Sequencing and computational approaches to identification and characterization of microbial organisms, *Biomed. Eng. Comput. Biol.* 5 (2013), <https://doi.org/10.4137/beeb.s10886> p. BECB. S10886.
- [6] S.J. Park, S. Onizuka, M. Seki, Y. Suzuki, T. Iwata, K. Nakai, A systematic sequencing-based approach for microbial contaminant detection and functional inference, *BMC Biol.* 17 (1) (2019) 72, <https://doi.org/10.1186/s12915-019-0690-0>.
- [7] C.W. Brasher, A. DePaola, D.D. Jones, A.K. Bej, Detection of microbial pathogens in shellfish with multiplex PCR, *Curr. Microbiol.* 37 (2) (1998) 101–107, <https://doi.org/10.1007/s002849900346>.

- [8] G.M. Wyatt, M.N. Langley, H.A. Lee, M.R.A. Morgan, Further studies on the feasibility of one-day Salmonella detection by enzyme-linked immunosorbent assay, *Appl. Environ. Microbiol.* 59 (5) (1993) 1383–1390.
- [9] X. Mao, L. Yang, X.L. Su, Y. Li, A nanoparticle amplification based quartz crystal microbalance DNA sensor for detection of *Escherichia coli* O157:H7, *Biosens. Bioelectron.* 21 (7) (2006) 1178–1185, <https://doi.org/10.1016/j.bios.2005.04.021>.
- [10] K. Shirasu, The HSP90-SGT1 chaperone complex for NLR immune sensors, *Annu. Rev. Plant Biol.* 60 (1) (2009) 139–164, <https://doi.org/10.1146/annurev.arplant.59.032607.092906>.
- [11] K. Yamanaka, et al., Quantitative detection for porphyromonas gingivalis in tooth pocket and saliva by portable electrochemical DNA sensor linked with PCR, *Electroanalysis* 26 (12) (2014) 2686–2692, <https://doi.org/10.1002/elan.201400447>.
- [12] A.N. Naimushin, S.D. Soelberg, D.U. Bartholomew, J.L. Elkind, C.E. Furlong, A portable surface plasmon resonance (SPR) sensor system with temperature regulation, *Sensors Actuators, B Chem.* 96 (1–2) (2003) 253–260, [https://doi.org/10.1016/S0925-4005\(03\)00533-1](https://doi.org/10.1016/S0925-4005(03)00533-1).
- [13] M.L. Pourciel-Gouzy, W. Sant, I. Humenyuk, L. Malaquin, X. Dollat, P. Temple-Boyer, Development of pH-ISFET sensors for the detection of bacterial activity, *Sensors Actuators, B Chem.* 103 (1–2) (2004) 247–251, <https://doi.org/10.1016/j.snb.2004.04.056>.
- [14] Y.-C. Lu, et al., Bacteria detection utilizing electrical conductivity, *Biosens. Bioelectron.* 23 (2008) 1856–1861, <https://doi.org/10.1016/j.bios.2008.03.005>.
- [15] R. Mempo, H. Tran, C. Chen, H. Gong, K. Kim Ho, S. Lu, Release of extracellular ATP by bacteria during growth, *BMC Microbiol.* 13 (1) (2013) 1–13, <https://doi.org/10.1186/1471-2180-13-301>.
- [16] K. Richter, M. Schicklberger, J. Gescher, Dissimilatory reduction of extracellular electron acceptors in anaerobic respiration, *Appl. Environ. Microbiol.* 78 (4) (2012) 913–921, <https://doi.org/10.1128/AEM.06803-11>.
- [17] K.L. Straub, M. Benz, B. Schink, Iron metabolism in anoxic environments at near neutral pH, *FEMS Microbiol. Ecol.* 34 (3) (2001) 181–186, [https://doi.org/10.1016/S0168-6496\(00\)00088-X](https://doi.org/10.1016/S0168-6496(00)00088-X).
- [18] M.P. Buttner, P. Cruz, L.D. Stetzenbach, A.K. Klima-Comba, V.L. Stevens, P.A. Emanuel, Evaluation of the biological sampling kit (BiSKit) for large-area surface sampling, *Appl. Environ. Microbiol.* 70 (12) (2004) 7040–7045, <https://doi.org/10.1128/AEM.70.12.7040-7045.2004>.
- [19] M. Salat, P. Petkova, J. Hoyo, I. Perelshtein, A. Gedanken, T. Tzanov, Durable antimicrobial cotton textiles coated sonochemically with ZnO nanoparticles embedded in an in-situ enzymatically generated bioadhesive, *Carbohydr. Polym.* 189, (November) 2017, 198–203, 2018, [10.1016/j.carbpol.2018.02.033](https://doi.org/10.1016/j.carbpol.2018.02.033).
- [20] J. Beddow et al., Sonochemical coating of textile fabrics with antibacterial nanoparticles, *AIP Conf. Proc.*, vol. 1433, no. May 2014, pp. 400–403, 2012, doi: 10.1063/1.3703213.
- [21] I. Perelshtein, et al., Making the hospital a safer place by sonochemical coating of all its textiles with antibacterial nanoparticles, *Ultrason. Sonochem.* 25 (2015) 82–88, <https://doi.org/10.1016/j.ultsonch.2014.12.012>.
- [22] P. Petkova, A. Francesko, I. Perelshtein, A. Gedanken, T. Tzanov, Simultaneous sonochemical-enzymatic coating of medical textiles with antibacterial ZnO nanoparticles, *Ultrason. Sonochem.* 29 (2016) 244–250, <https://doi.org/10.1016/j.ultsonch.2015.09.021>.
- [23] I. Perelshtein, A. Lipovsky, N. Perkas, T. Tzanov, A. Gedanken, Sonochemical coposition of antibacterial nanoparticles and dyes on textiles, *Beilstein J. Nanotechnol.* 7 (1) (2016) 1–8, <https://doi.org/10.3762/bjnano.7.1>.
- [24] C. Gervais, et al., Why does Prussian blue fade? understanding the role(s) of the substrate, *J. Anal. At. Spectrom.* 28 (10) (2013) 1600–1609, <https://doi.org/10.1039/c3ja50025j>.
- [25] P. Ertl, B. Unterladstaetter, K. Bayer, S.R. Mikkelsen, Ferricyanide reduction by *Escherichia coli*: Kinetics, mechanism, and application to the optimization of recombinant fermentations, *Anal. Chem.* 72 (20) (2000) 4949–4956, <https://doi.org/10.1021/ac000358d>.
- [26] D.R. Rosseinsky, L. Glasser, H.D.B. Jenkins, Thermodynamic clarification of the curious ferric/potassium ion exchange accompanying the electrochromic redox reactions of Prussian Blue, iron(III) hexacyanoferrate(II), *J. Am. Chem. Soc.* 126 (33) (2004) 10472–10477, <https://doi.org/10.1021/ja040055r>.
- [27] P. Ding, G. Song, J. Zhou, Q. Song, Collection of rolling fingerprints by the electrochromism of Prussian blue, *Dye. Pigment.* 120 (2015) 169–174, <https://doi.org/10.1016/j.dyepig.2015.04.019>.
- [28] F. Ricci, G. Pallechi, Sensor and biosensor preparation, optimisation and applications of Prussian Blue modified electrodes, *Biosens. Bioelectron.* 21 (3) (2005) 389–407, <https://doi.org/10.1016/j.bios.2004.12.001>.
- [29] P.A. Fiorito, V.R. Gonçalves, E.A. Ponzio, S.I. Córdoba De Torresi, Synthesis, characterization and immobilization of Prussian blue nanoparticles. A potential tool for biosensing devices, *Chem. Commun.* no. 3 (2005) 366–368, <https://doi.org/10.1039/b412583e>.
- [30] A.A. Karyakin, Advances of Prussian blue and its analogues in (bio)sensors, *Curr. Opin. Electrochem.* 5 (1) (2017) 92–98, <https://doi.org/10.1016/j.coelec.2017.07.006>.
- [31] M.K. Jahn, S.B. Haderlein, R.U. Meckenstock, Reduction of Prussian Blue by the two iron-reducing microorganisms *Geobacter metallireducens* and *Shewanella alga*, *Environ. Microbiol.* 8 (2) (2006) 362–367, <https://doi.org/10.1111/j.1462-2920.2005.00902.x>.
- [32] D. Ellis, M. Eckhoff, V.D. Neff, Electrochromism in the mixed-valence hexacyanides. I. Voltammetric and spectral studies of the oxidation and reduction of thin films of Prussian blue, *J. Phys. Chem.* 85 (9) (1981) 1225–1231, <https://doi.org/10.1021/j150609a026>.

- [33] A.A. Karyakin, Prussian Blue and its analogues: electrochemistry and analytical applications, *Electroanal.* 13 (10) (2001) 813–819, [https://doi.org/10.1002/1521-4109\(200106\)13:10<813::AID-ELAN813>3.0.CO;2-Z](https://doi.org/10.1002/1521-4109(200106)13:10<813::AID-ELAN813>3.0.CO;2-Z).
- [34] D. Davidson, L.A. Welo, The nature of prussian blue, *J. Phys. Chem.* 32 (8) (1928) 1191–1196, <https://doi.org/10.1021/j150290a007>.
- [35] C. Gervais, M. A. Languille, S. Reguer, C. Garnier, M. Gillet, Light and anoxia fading of Prussian blue dyed textiles, *Herit. Sci.*, vol. 2, no. 1, 2014, doi: 10.1186/s40494-014-0026-x.
- [36] P. Petkova, et al., Sonochemical coating of textiles with hybrid ZnO/chitosan antimicrobial nanoparticles, *ACS Appl. Mater. Interfaces* 6 (2) (2014) 1164–1172, <https://doi.org/10.1021/am404852d>.
- [37] A. Alonso, et al., Superparamagnetic Ag@Co-nanocomposites on granulated cation exchange polymeric matrices with enhanced antibacterial activity for the environmentally safe purification of water, *Adv. Funct. Mater.* 23 (19) (2013) 2450–2458, <https://doi.org/10.1002/adfm.201202663>.
- [38] I. Perelshtein, et al., CuO-cotton nanocomposite: formation, morphology, and antibacterial activity, *Surf. Coatings Technol.* 204 (1–2) (2009) 54–57, <https://doi.org/10.1016/j.surfcoat.2009.06.028>.
- [39] T. Harifi, M. Montazer, A review on textile sonoprocessing: a special focus on sonosynthesis of nanomaterials on textile substrates, *Ultrason. Sonochem.* 23 (2015) 1–10, <https://doi.org/10.1016/j.ultsonch.2014.08.022>.
- [40] M. Cheng, et al., In situ formation of pH-responsive Prussian blue for photoacoustic imaging and photothermal therapy of cancer, *RSC Adv.* 7 (30) (2017) 18270–18276, <https://doi.org/10.1039/C7RA01879G>.
- [41] Hatamie, Amir, Zargar, Behrooz, A. Jalali, H. Ameri, Colorimetric assay for 4-phenylthiosemicarbazide detection in environmental samples based on Prussian Blue nanoparticles formation ion, *Iran. J. Chem. Chem. Eng.* 36 (1), 2017.
- [42] B. Zargar, A. Hatamie, Prussian blue nanoparticles: A simple and fast optical sensor for colorimetric detection of hydralazine in pharmaceutical samples, *Anal. Methods* 6 (15) (2014) 5951–5956, <https://doi.org/10.1039/c4ay00618f>.
- [43] A.J. Bard, L.R. Faulkner, E. Swain, C. Robey, *Electrochemical Methods. Fundamentals and Applications*, 1980.
- [44] F. Kracke, I. Vassilev, J.O. Krömer, Microbial electron transport and energy conservation – The foundation for optimizing bioelectrochemical systems, *Front. Microbiol.*, 6 (JUN), 1–18, 2015, doi: 10.3389/fmicb.2015.00575.
- [45] K. Catterall, D. Robertson, P.R. Teasdale, D.T. Welsh, R. John, Evaluating use of ferricyanide-mediated respiration bioassays to quantify stimulatory and inhibitory effects on *Escherichia coli* populations, *Talanta* 80 (5) (2010) 1980–1985, <https://doi.org/10.1016/j.talanta.2009.10.057>.
- [46] G. Pankratova, L. Hederstedt, L. Gorton, Extracellular electron transfer features of Gram-positive bacteria, *Anal. Chim. Acta* 1076 (2019) 32–47, <https://doi.org/10.1016/j.aca.2019.05.007>.